

# TOPEX Microwave Radiometer Thermal Control: Post-System-Test Modifications and On-Orbit Performance

Edward I. Lin\*

*Jet Propulsion Laboratory, California Institute of Technology, Pasadena, California 91109*

The TOPEX spacecraft thermal vacuum test revealed that its Microwave Radiometer instrument thermal design neglected a shading condition, causing the model prediction of a key electronics temperature to be 7.5°C higher than the test result. The thermal model and hardware were modified right before launch to correct for the design inadequacy. This paper reports on how the initially obscure problem was discovered, and how the thermal models were revised, validated, and utilized to investigate the solution options and guide the hardware modification decisions. Details related to test data interpretation, analytical uncertainties, and model-prediction vs. test-data correlation are documented. Instrument/spacecraft interface issues, where the problem originated and where in general pitfalls abound, are dealt with specifically. Finally, on-orbit thermal performance data are presented, which exhibit good agreement with flight predictions, and which indicate comfortable temperature margins. Namely, the key electronics temperature is 10°C below the maximum flight allowable during the hot operating mode, and 5°C above the minimum flight allowable during the cold operating mode. Lessons learned on the way to attaining this excellent thermal performance are discussed.

## Introduction

THE TOPEX/POSEIDON spacecraft was launched on August 10, 1992, from Kourou, French Guiana, by an Ariane 42P rocket to study the earth oceanic circulation and dynamics. Orbiting the earth at an altitude of 1336 km with an inclination of 66 deg, the satellite has been functioning extremely well. The TOPEX Microwave Radiometer (TMR), as shown in Fig. 1, determines the water-vapor content in the troposphere, which is used to improve the accuracy of the sea-surface height measured by radar altimetry. It consists of an antenna, a RF shield, and the main chassis, which houses the electronics, wave guides, feed horn, and calibration horns. The instrument is mounted on the spacecraft with six titanium struts, is equipped with survival heaters, and relies on two louvered radiators to dissipate a major portion of the 24-W operating power.

The TOPEX system thermal vacuum test was conducted at the Goddard Space Flight Center (GSFC) facilities. The spacecraft test configuration is shown in Fig. 2. The TMR participated in the test without the antenna and the antenna base ring blanket, and with two test targets, which were not part of the flight hardware but which were present for performance evaluation purposes (Figs. 2 and 3). The spacecraft was divided into a dozen thermal-control zones, and each zone was provided with a plate shroud, which was temperature-controlled by the circulating liquid/gaseous nitrogen to simulate the radiation environment. The TMR was assigned two zones, 8A and 8B (Fig. 3). The zone shrouds, together with the vacuum-chamber walls, were controlled to predetermined effective sink temperatures during various phases of the test.

For the TMR, the test results were positive in several respects: the survival heaters functioned properly, the louvers opened within the expected temperature range, and test data for the hot-balance test phases agreed well with model predictions. However, a large discrepancy was noticed between the cold-balance test data and the predictions made by a 20-node reduced model. This started a chain of events that included explaining the discrepancy, uncovering the thermal-design inadequacy, investigating the solution options,

selecting the most practical and low-risk approaches to modify the hardware, and finally implementing the solution. All of this took place within a month and just in time for shipping the spacecraft to the launch site.

This paper documents these activities and the important technical deliberations that led to the discovery of the thermal-design problem as well as the solution. It also reports on inflight thermal performance of the TMR, which has proven to be excellent, attesting the validity of the hardware modifications and all the preceding analyses.

## Discovery of the Shading Problem

During the cold-balance test, two concerns surfaced. First, the temperature for the Ch 1&4 RF module (or Word 29), a representative electronics temperature, was observed to be 0.9°C. This was significantly lower than the 18°C predicted by the spacecraft contractor (Fairchild Space) using a 20-node reduced model. This large discrepancy, and the fact that the electronics were below the 10°C allowable flight limit (later revised to 5°C), raised a serious concern. Second, the survival heaters were activated too frequently during the test. Although this was a positive indication that the survival heaters were responsive and would be able to prevent the electronics from falling below 0°C in flight, as intended by design, the frequent on-off switching of the survival heaters might have undesirable effect on TMR data quality.

Regarding the first concern, it was quickly pointed out that the 20-node reduced model for the test configuration (provided by JPL and integrated by Fairchild into the spacecraft model) was never validated, because there were no test data available for validation prior to the system test. Nor was there a detailed model for the test configuration that could be used as a comparison. Therefore the 20-node model prediction was questionable and could not be relied upon as the basis of comparison. Consequently, in order to explain the discrepancy and to understand the reasons for the low electronics temperatures, the JPL detailed TRASYS and SINDA models for TMR (248 nodes) were adapted for the test configuration, incorporating the test targets, the zone-8 shrouds, and the vacuum chamber (see Figs. 2 and 3). These then became the test models and were used throughout the test for data correlation and interpretation.

The results of correlation between the model predictions and test data for eight test cases are summarized in Table 1 (the three JPL test cases have been detailed in Ref. 1). The Table 1 results remained valid prior to the discovery of the shading problem (described below). As can be seen in Table 1, all the hot and "mild" cases (i.e., cases 1 through 6) display good agreement between predictions and data. However, significant discrepancies exist for the cold cases

Received May 27, 1993; presented as Paper 93-2743 at the AIAA 28th Thermophysics Conference, Orlando, FL, July 6–9, 1993; revision received Jan. 23, 1994; accepted for publication Feb. 24, 1994. Copyright © 1994 by the American Institute of Aeronautics and Astronautics, Inc. No copyright is asserted in the United States under Title 17, U.S. Code. The U.S. Government has a royalty-free license to exercise all rights under the copyright claimed herein for Governmental purposes. All other rights are reserved by the copyright owner.

\*Member of Technical Staff. Member AIAA.

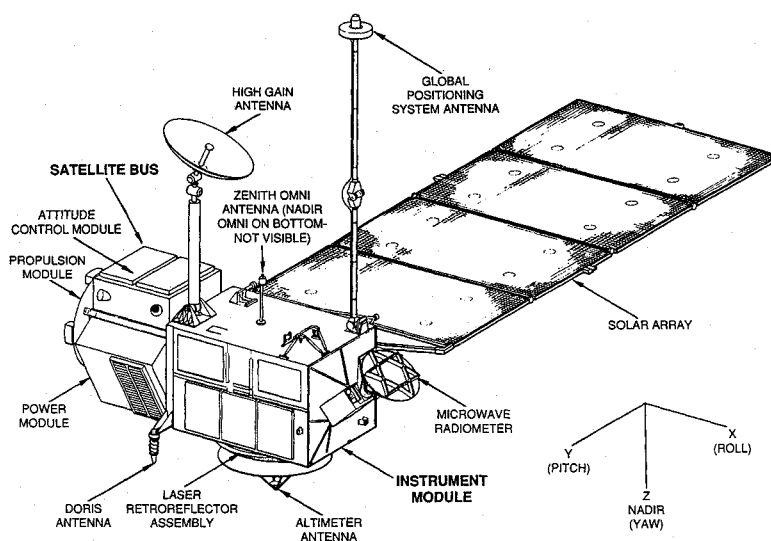


Fig. 1 The TOPEX/POSEIDON satellite.

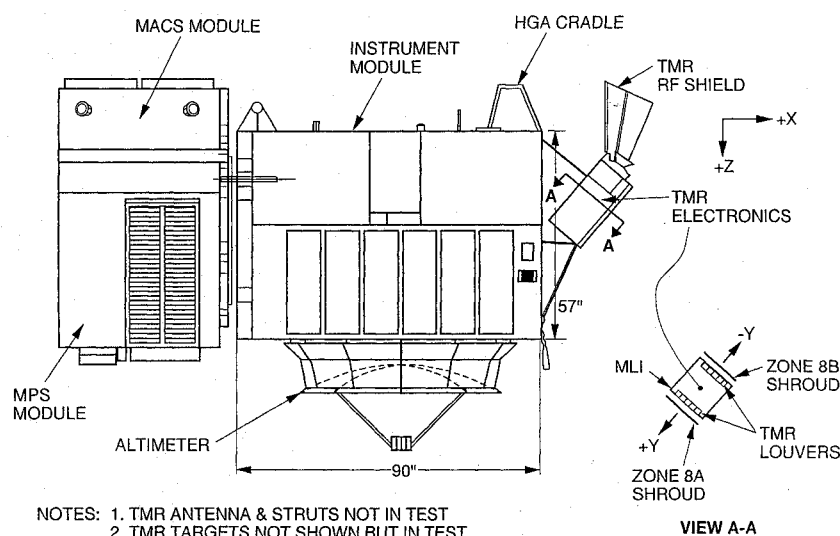


Fig. 2 TOPEX thermal vacuum test configuration (TMR mounted on the +X face of the instrument module).

(i.e., cases 7 and 8, where the chamber wall temperature was below  $-50^{\circ}\text{C}$ ). Incidentally, note that in case 7, which was the first cold-balance case to raise concerns, the detailed test model predicted  $8.4^{\circ}\text{C}$  for the electronics. This was a substantial improvement over the 20-node model's prediction of  $18^{\circ}\text{C}$  mentioned above. However, the discrepancy of  $7.5^{\circ}\text{C}$  against the data was still troublesome, particularly when viewed together with case 8.

Regarding the second concern, it was noted that the zone-8 shrouds were operated at  $-185^{\circ}\text{C}$  during the cold-balance test. This caused the louver and radiator temperatures to be low (near  $0^{\circ}\text{C}$ ) because the shrouds were only 2 or 3 cm away from the louvers. The survival heaters were mounted on the inside of the radiators, and were duly activated by the low radiator temperatures. However, based on effective sink temperatures calculated using flight fluxes obtained from the TRASYS model, the louvers and radiators should face a significantly warmer external environment in flight than the  $-185^{\circ}\text{C}$  shrouds. Therefore, their temperatures should be higher, and the anomaly of frequent activation of the survival heaters should be unlikely during flight. This would be especially true if the electronics temperatures were also higher than observed. Thus both concerns boiled down to the same question, and it was imperative that the causes for the low electronics temperatures be determined.

Fairchild had determined the chamber wall temperatures according to conditions pertinent to the altimeter and the +Z surfaces (see Fig. 2). These conditions are not exactly the same as for the TMR.

The RF shield temperature had always tracked the chamber wall temperature closely, both in the JPL thermal balance test and the GSFC system thermal test. This meant that during the cold balance tests the RF shield temperature was around  $-50^{\circ}\text{C}$ , which was in distinct contrast with previous flight predictions of around  $-15^{\circ}\text{C}$ . The much lower temperature of the RF shield could certainly drive down the electronics temperatures, because the RF shield was hard-mounted to the TMR chassis and the six aluminum struts would serve as a good conductor of heat from the chassis to the shield. Could it be that the effective sink temperatures employed for the chamber wall and the zone-8 shrouds were much too low for the TMR?

Radiant flux comparisons were then made between JPL and Fairchild. It was found that JPL and Fairchild had used exactly the same input flux parameters to the TRASYS program for both the hot and cold orbits. Also, JPL and Fairchild agreed on the absorbed heat fluxes used for the louvered radiator surfaces. The possibility of shading of the TMR by the high-gain antenna (HGA) was suggested by Fairchild, but at  $\beta = 88^{\circ}$  ( $\beta$  being the angle between the sun vector and the orbit plane), this appeared to be either unlikely or insignificant. Finally, shading by the MACS module (modular attitude-control subsystem; see Fig. 2) was brought to light. Fairchild faxed JPL two drawings that indicate that the TMR is shaded by the MACS module in the vicinity of  $\beta = 88^{\circ}$  (in terms of Fig. 2, the sun would be coming nearly horizontally from the left).

**Table 1** Interim correlation of TMR model predictions with test data<sup>a</sup> (before the shading problem was discovered)

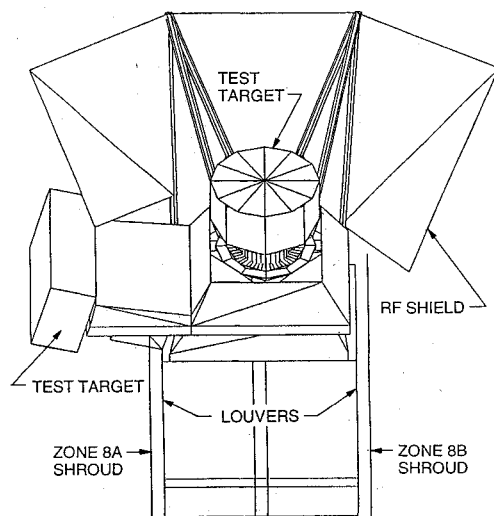
Test Case	Chamber wall T, °C	Louver shroud T, °C	Electronics Temp., °C			Test site <sup>c</sup>	Remark
			Model pred.	Test data	$\Delta T$		
1	20	-58	28.8	27.1	1.7	GSFC	1st hot balance
2	21	-4	35.1	37.8	-2.7	GSFC	2nd hot balance
3	2	-190	-2.8	1.2	-4.0	GSFC	Survival heater test
4	0	N/A	29.4	28.3	1.1	JPL	Hot steady state
5	-10	N/A	23.7	20.9	2.8	JPL	Cold steady state
6	-33	N/A	1.9	2.2	-0.3	JPL	Survival mode
7	-50	-185	8.4	0.9	7.5	GSFC	1st cold balance
8	-57	0	21.1	11.0	10.1	GSFC	2nd cold balance

<sup>a</sup>The old rf shield model and a blanket effective emittance of 0.015 were used in the detailed models.

<sup>b</sup>Ch 1&4 rf module (1A3) temperature, model prediction given by SINDA node 3111, test data given by Word 29;

$\Delta T = T_{\text{pred}} - T_{\text{test}}$ .

<sup>c</sup>System-level (satellite) test was done at GSFC (March–April 1992), and subsystem-level (TMR only) test was done at JPL (September 1990).

**Fig. 3** Plot of the TRASYS model for the TMR test configuration.

The MACS shading would be significant, as it would mean that the effective sink temperatures used in the tests were probably not too low for the TMR. It would also mean that the RF shield would be much colder than previously predicted, as the MACS shading was not allowed for in the TRASYS model up till then. The MACS shading problem was confirmed when Fairchild provided satellite dimensions pertinent to the issue.

An examination of a TRASYS cold-orbit run revealed that without the MACS shading, the direct solar load on the RF shield was 142 W, and the albedo plus earth heat load was 17 W; i.e., direct solar was 89% of total. Without shading, the direct solar component had contributed much to warm the RF shield to about  $-15^{\circ}\text{C}$ . With shading, direct solar being blocked, the RF shield temperature went down to about  $-100^{\circ}\text{C}$ . The nature of the problem was now clear, and the causes for the low electronics temperatures found. In flight, the MACS shading in the neighborhood of  $\beta = 88$  deg would cause the RF shield to go very cold, and the black-painted aluminum shield and struts would serve as a very effective radiator to dissipate large amounts of heat, which would be easily conducted across the struts because of the large temperature gradient set up between the TMR chassis and the RF shield.

### Thermal Model Modifications and Validation

To resolve the shading problem, the thermal models had to be modified. A rectangular surface was first added to the TRASYS model to account for the MACS shading at  $\beta = 88$  deg and vicinity. In the meantime, two additional pieces of information emerged which had an important effect on the assessment being made.

First, two of the six RF shield struts (the "lower" ones that are best connected to the shield) had a thickness of 0.049 in. instead of

the 0.030 in. previously communicated to the thermal engineer. This meant that the cross-sectional areas for these tubes, and hence their conductances, were actually 59% greater than had been modeled. Second, the TMR will be shaded (by the MACS or the HGA) for a substantial portion of its functional life. This assessment is supported by a TOPEX satellite yaw maneuver packet which was previously unavailable to the thermal engineer. This packet indicates that  $\beta = 30$  to  $40$  deg has the highest probability of occurrence, and that at  $\beta = 40$  deg, as at other angles, the spacecraft yaw maneuver will be such as to cause the TMR to be shaded most of the time. The implication of this is that the TMR should really be designed more for the cold orbits than for the hot orbits, contrary to previous emphasis.

Thus, it became clear that a careful reexamination must be made of the RF shield design, and the shield might have to be reworked. More details were therefore added to enhance the shield representation. In all, 6 nodes were added to the TRASYS model, and 16 nodes and 27 conductive conductors to the SINDA model.

Another round of model/test correlation was performed subsequent to the model modifications, resulting in Table 2. Besides taking account of some details of the test targets that were not part of the flight models, two additional adjustments to the models were necessary to bring the predictions to closer agreement with the cold-balance data (cases 7 and 8). First, a blanket effective emittance of 0.03 was used instead of 0.015. Second, the conductance between the RF cover and the top-hat support in the 4-bolt mounting area was adjusted upward somewhat. Several significant points are to be noted in comparing Tables 1 and 2 and in interpreting these results:

1) The old RF shield model would have been adequate if the MACS shading were not a problem. Cases 1 and 2 show that the new RF shield model and the higher blanket effective emittance make little difference for the temperature predictions. The JPL test cases were not rerun, but the fact that the RF shield temperatures were mild in these tests (and therefore the  $\Delta T$  between the shield and the chassis were relatively small) would argue for similar results.

2) Out of all the test cases listed in Table 2, case 7, with the noted effective sink temperatures, best reflects the MACS shading conditions and provides the best simulation of actual cold orbits for the TMR. The new RF shield model and  $\epsilon_{\text{eff}} = 0.03$  have a significant effect on the predicted electronics temperature ( $0.9^{\circ}\text{C}$  vs the previous  $8.4^{\circ}\text{C}$ ). The same is true for case 8, although a zone 8 shroud temperature equal to  $0^{\circ}\text{C}$  most probably would not represent any real cold-orbit conditions.

3) An inspection of the raw test data indicated that case 8 probably did not reach steady state. A smaller  $\Delta T$  would be expected when steady-state is reached. As for case 3, the steady-state analytical treatment of the transient, cyclic situation was approximate. The test data of  $1.2^{\circ}\text{C}$  were an average; the cycling of the heater power was treated by an averaging method based on the on-off periods; and the nodal distribution of the average power was done expeditiously to save time. The  $\Delta T$  of  $-7.6^{\circ}\text{C}$  (although not necessarily regarded as excessive by normal standards) was partially attributable to these

**Table 2 Final correlation of TMR model predictions with test data<sup>a</sup> (after the shading problem was discovered and the model was corrected)**

Test Case	Chamber wall T, °C	Louver shroud T, °C	Electronics Temp., °C			Test site <sup>c</sup>	Remark
			Model pred.	Test data	$\Delta T$		
1	20	-58	28.8	27.1	1.7	GSFC	1st hot balance
2	21	-4	36.3	37.8	-1.5	GSFC	2nd hot balance
3	2	-190	-6.4	1.2	-7.6	GSFC	Survival heater test
4	0	N/A	29.4	28.3	1.1	JPL	Hot steady state
5	-10	N/A	23.7	20.9	2.8	JPL	Cold steady state
6	-33	N/A	1.9	2.2	-0.3	JPL	Survival mode
7	-50	-185	0.9	0.9	0.0	GSFC	1st cold balance
8	-57	0	17.8	11.0	6.8	GSFC	2nd cold balance

<sup>a</sup>The new RF shield model and a blanket effective emittance of 0.03 were used in the detailed models.

<sup>b</sup>Ch 1&4 RF module (1A3) temperature, model prediction given by SINDA node 3111, test data given by Word 29;

$\Delta T = T_{\text{pred}} - T_{\text{test}}$ .

<sup>c</sup>System-level (satellite) test was done at GSFC (March–April 1992), and subsystem-level (TMR only) test was done at JPL (September 1990).

**Table 3 TMR hardware modification options analyzed**

Case 1.	Baseline (no hardware modification)—cold case with MACS shading <sup>a</sup>
Case 2.	Case 1 + blanket on back side of shield <sup>b</sup>
Case 3.	Case 2 + Al tape on struts + front side of shield painted with D4D ( $\alpha/\epsilon = 0.3/0.3$ )
Case 4.	Case 2 + Al tape on struts + paint removed from front side of shield, and surface sanded <sup>c</sup>
Case 5.	Case 4 + G10 washer and Ti fitting on 2 lower struts
Case 6.	Case 5 + G10 washer and Ti fitting on 2 upper struts
Case 7.	Case 6 + replacement of 6 in. of bipod with Ti tubes
Case 8.	Case 7 + replacement of 6 in. of 2 upper struts with Ti tubes
Case 9.	Case 5 + complete coverage of -Y-side louver with MLI
Case 10.	Case 5 + partial coverage (71%) of -Y-side louver with MLI

<sup>a</sup>A rectangular surface was incorporated into TRASYS to model shading by the MACS.

<sup>b</sup>Twenty layers; cases 1 to 8,  $\epsilon_{\text{eff}} = 0.015$ , cases 9 and 10,  $\epsilon_{\text{eff}} = 0.03$ .

<sup>c</sup>Measured optical properties for the exposed aluminum surface are  $\alpha/\epsilon = 0.16/0.04$ .

approximations, but a more exact treatment of the transient, cyclic situation would have been very time-consuming.

To summarize the discovery of the shading problem and the correction process for the thermal models, it is noted that a large temperature discrepancy was first indicated by a comparison between the test data and the reduced-model predictions. Subsequent use of the detailed models improved the predictions and confirmed the discrepancy. The discrepancy was considerable only for two cold cases; for the remaining six test cases, good agreement was evident between the analytical and test results (Table 1). Two questions were raised at that point: Was the model done properly for the cold cases? Were the effective sink test temperatures (an approximate boundary-condition simulation approach) properly specified? It turned out that the effective sink temperatures were largely justified by the condition of the MACS shading on the TMR, and that the model was inadequate as a result of the missing key information and hot-biased design approach. The discovery of the shading problem and the correction of the model to allow for the shading led to the improved correlation results shown in Table 2. These results are quite satisfactory, in view of the above discussion, and the thermal models so validated are considered to be adequate for use in making flight predictions and in guiding the hardware modification effort.

### Investigation of Solution Options

Once the MACS shading and the RF shield design were ascertained to be the causes for the unacceptably low electronics temperatures, the solution was obvious. The RF shield must be conductively decoupled from the TMR chassis or at least rendered ineffective as a radiator. One of the first simulations performed to explore solution options involved replacing all the aluminum struts by titanium ones. With thermal conductivity almost 40 times lower than aluminum, the titanium struts were shown to effectively isolate the RF shield from the TMR chassis. Consequently, whatever happens to the RF shield thermally will not matter much to the electronics. However, extensive discussions involving hardware, project, reliability, and instrument personnel (both Fairchild and JPL) led to the conclusion

**Table 4 TMR temperature predictions (°C) associated with hardware modification options as defined in Table 3**

Case	Electronics		RF Shield	
	Ch 1&4 Mod (node 3111)	Data Module (node 3126)	Al shield	Back-side MLI
1	-8.4	-11.8	-132.0	N/A
2	1.1	-1.8	-71.8	-140.1
3	6.9	4.2	-61.3	-140.2
4	8.4	5.9	-50.1	-138.3
5	12.1	9.9	-60.2	-140.0
5 <sup>a</sup>	6.5	3.8	-61.8	-138.7
6	13.2	10.9	-63.4	-140.1
7	14.9	12.8	-68.9	-141.2
8	15.4	13.2	-71.5	-141.6
9	17.2 <sup>b</sup>	14.6	-57.7	-138.7
10	13.9 <sup>c</sup>	11.3	-59.2	-138.7

<sup>a</sup>This case has the same hardware modifications as case 5 except for the following adjustments in the model: 1) the MLI effective emittance is 0.03 instead of 0.015; 2) conductance is adjusted between the RF cover and top-hat support.

<sup>b</sup>The corresponding temperature for the hot case is 36.8°.

<sup>c</sup>the corresponding temperature for the hot case is 28.6°.

that this approach was not feasible within the known time constraint. A series of alternative options were then investigated, and most of them served to reduce the RF shield's ability to radiate heat.

Table 3 lists the options analyzed, and Table 4 presents the results obtained. It is seen that significant temperature improvements are obtainable by installing a multilayer insulation (MLI) blanket on the back side of the RF shield (9.5°C), by removing the black paint from the front side of the shield and wrapping the struts with aluminum tape (7.3°C), and by replacing the aluminum fittings with titanium fittings and G10 washers on the two lower struts (3.7°C). Cases 6, 7, and 8 contribute additional gains that are less dramatic than cases 2 through 5. Therefore, a team decision was made to adopt case 5 as a baseline for implementation. Case 5 predicted, as shown in Table 4, 12.1°C for the key electronics temperature, which was 2°C above the allowable lower limit.

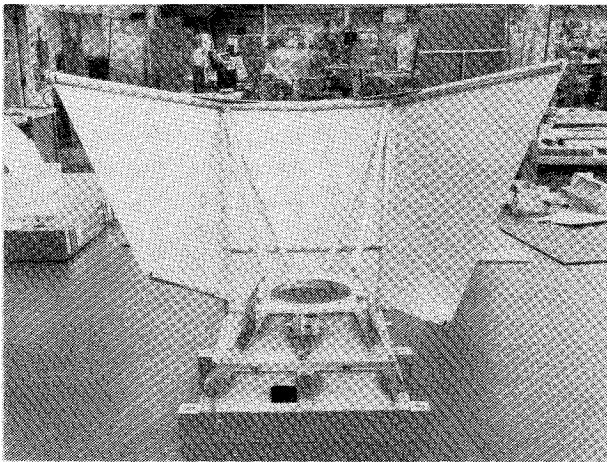


Fig. 4 TMR RF shield with its six supporting struts.

However, a subsequent sensitivity study varying the blanket effective emittance indicated that the predicted  $12.1^{\circ}\text{C}$  for case 5 could be lowered significantly, to  $6.5^{\circ}\text{C}$  as shown in case 5' (Table 4), if we took  $\epsilon_{\text{eff}} = 0.03$  (instead of 0.015) and if the conductance between the RF cover and the top-hat support was adjusted, as consistent with the final round of model/test correlation, which yielded Table 2. Furthermore, information that emerged at this juncture indicated that the TMR would face a cold environment more often than not (as stated in the previous section). Naturally, a prudent step to take at this point was to seek further improvement that could be implemented within the existing time constraints. Cases 9 and 10 were then studied. They involved covering the  $-Y$ -side louver with a 20-layer MLI—fully and partially, respectively. Case 10, with 71% of the louver covered, yielded the most attractive results:  $13.9^{\circ}\text{C}$  for the electronics in the cold case and  $28.6^{\circ}\text{C}$  in the hot case (flight allowables given in a later table).

Note that proper conservatism was exercised in all these analyses. For example, although the actual uncovered (or exposed) louver length is 3.7 in., it was represented in the model as 4.45 in. This was done to allow for additional exposure of the louver blades to space due to such deviation from idealization as gaps, a shallow-angle view factor, etc. On the hot side, a parametric study was made where the exposed louver area was arbitrarily reduced by 38%. This raised the electronics temperature to  $30.5^{\circ}\text{C}$  from  $28.6^{\circ}\text{C}$ . The point of a partially covered louver is that it can still regulate the emissivity so as to prevent excessively high temperature on the hot side (cf. cases 9 and 10).

### Hardware Modifications

All the recommended hardware modifications were implemented. These included the following (see Fig. 4 for a picture of the RF shield):

- 1) Removed all black paint from the RF shield, front and back surfaces, including the struts. The optical properties of the exposed aluminum surface were measured:  $\alpha/\epsilon = 0.16/0.04$ .
- 2) Installed a 20-layer MLI on the back side of the RF shield.
- 3) Replaced two lower aluminum tube fittings with titanium fittings and G10 washers.
- 4) Covered 71% of the  $-Y$ -side louver with a 20-layer MLI. The existing holes on the louver frame accommodated this readily.

### Flight Predictions and Uncertainties

With these hardware modifications incorporated in the detailed TRASYS and SINDA models, the predicted steady-state temperatures for the Ch 1&4 RF module during the hot and cold orbits are:

	Flight prediction	Allowable limit
Hot-orbit max.	$29^{\circ}\text{C}$	$40^{\circ}\text{C}$
Cold-orbit min.	$14^{\circ}\text{C}$	$5^{\circ}\text{C}$

The allowable operating limits shown above are results of a revision following a careful assessment by the project and instru-

ment personnel. (The previous allowable operating range was 10 to  $35^{\circ}\text{C}$ .)

The margins are thus seen to be  $11^{\circ}\text{C}$  on the hot side, and  $9^{\circ}\text{C}$  on the cold side. These appear to be comfortable margins to allow for uncertainties that may arise from various sources: e.g., the test configuration being non-flight-like, potential changes in optical and thermophysical properties due to environmental effects, increased heat loads due to contamination, contact conductances and MLI effective emittance being imperfectly characterized, on-orbit anomalies requiring operational changes, and many other unknown factors. The assignment of uncertainty margins can be very subjective. Donabedian<sup>2</sup> reported a  $7^{\circ}\text{C}$  standard deviation between test-correlated model predictions and on-orbit temperature measurements for the Surveyor spacecraft, among other statistics. The TMR margins as indicated above exceed this value.

### On-Orbit Thermal Performance

Since TOPEX's launch, the thermal performance of the TMR, as well as of the entire spacecraft, has been very satisfactory. The on-orbit temperature history of a critical TMR electronic component (i.e., the Ch 1&4 RF module) is shown in Fig. 5. Throughout the first 158 days, the temperature has stayed well within the required operating minimum and maximum, exhibiting more than  $10^{\circ}\text{C}$  of margin on the hot side, and more than  $5^{\circ}\text{C}$  of margin on the cold side. The temperature peaks typically occurred during the periods when the spacecraft had a fixed-yaw attitude (i.e., days 30–40, 90–103, and 138–152), whereas low temperatures occurred when the spacecraft underwent a sinusoidal yaw maneuver. During the yaw maneuver (for  $|\beta| \geq 20^{\circ}$  roughly), the spacecraft is typically oriented so that the TMR faces away from the sun and is shaded from the back by the spacecraft, whence the lower temperatures. On the other hand, at low  $\beta$  angles (i.e.,  $|\beta| \leq 20^{\circ}$  roughly), the spacecraft does not yaw, and the TMR is exposed to the sun during a portion of the orbit, which explains the higher temperatures. Note that the temperature predictions for both the hot and cold steady states agree closely with on-orbit temperatures.

The temperature trend for the electronics (as exemplified by Fig. 5) is corroborated by temperatures for other parts of the TMR, for example, the multifrequency feed horn, as shown in Fig. 6. In

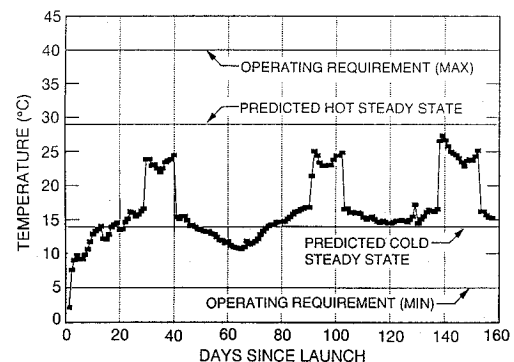


Fig. 5 On-orbit temperature history for the 21-GHz electronics (Dicke SW1).

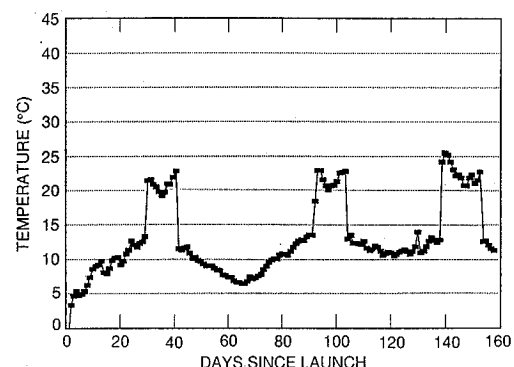


Fig. 6 On-orbit temperature history for the TMR multifrequency feed horn.

this case, however, no stringent temperature requirements are imposed. So far, the spacecraft has gone through a wide range of  $\beta$  angles ( $-80^\circ \leq \beta \leq +80^\circ$ ). Higher  $\beta$  angles (as high as  $\pm 88^\circ$ ) are expected to be encountered in 1995. However, it is not anticipated that this will result in any significantly lower temperatures than witnessed in the first 158 days. It is evident that the thermal design for the TMR will be adequate for the entire mission. It is also evident that the post-system-test hardware modifications were critical to this successful outcome. Had any of the recommended steps not been implemented (especially the last step of covering 71% of the  $-Y$ -side louver with MLI), the result would have been violation of the lower operating-temperature limit and loss of a considerable number of data.

### Conclusions

A well-planned and -executed thermal vacuum test is invaluable and indispensable. It is highly desirable to make the test configuration as flight-like as possible, but where circumstances preclude this, it is still possible to derive important information on the thermal behavior of an instrument (or spacecraft) from a careful analysis of the test data. The discovery of the TMR shading problem and its resolution provides such an example. The intensive correlation of test data with model predictions played an important part in this case, where the analytical models were validated by test data and subsequently utilized to guide the hardware modification decisions. The analytical predictions carry uncertainties, however, owing to numerous sources as discussed above. This is a fact of reality that must be appreciated, and reckoned with by a design as robust as practicable. Adequate uncertainty margins are invariably incorporated into a sound design.

Interface communication is crucial. In a complex project (such as TOPEX) where the instrument spacecraft interface means an interface between different companies (or different countries), and where interaction between various technical disciplines and administrative units is commonplace, pitfalls abound for communication to break down. Needless to say, a watchful eye, as well as an effective management approach, is needed to prevent things from falling through the cracks. The TMR experience has underscored the importance of interface communication most emphatically.

As of day 158, the on-orbit thermal performance of the TMR has been very satisfactory. By all indications, this should remain true for the rest of the mission.

### Acknowledgments

The work described in this paper was carried out by the Jet Propulsion Laboratory, California Institute of Technology, under a contract with the National Aeronautics and Space Administration. The author would like to thank J. Stultz, who provided technical advice and support, and a large number of individuals who contributed in various ways to make the TMR modification effort a success. The list includes R. Grippi, W. Ruff, R. Whitt, J. Real, H. VonDeldon, P. Olson, F. Soltis, J. Fu, R. Karam, F. DeMauro, R. Miyake, G. Siebes, J. Roschke, E. Kellum, T. Almaguer, A. Zieger, R. Collins, J. Hultberg, and many more. Helpful comments on the manuscript by J. Stultz and R. Reeve are also appreciated.

### References

- <sup>1</sup>Lin, E. I., "TOPEX Microwave Radiometer: Thermal Design Verification Test and Analytical Model Validation," AIAA Paper 92-0816, Jan. 1992.
- <sup>2</sup>Donabedian, M., "Thermal Uncertainty Margins for Cryogenic Sensor Systems," AIAA Paper 91-1426, June 1991.